Energy determinants GAPDH and NDPK act as genetic modifiers for hepatocyte inclusion formation

Natasha T. Snider,[1] Sujith V.W. Weerasinghe,[1] Amika Singla,[1] Jessica M. Leonard,[1] Shinichiro Hanada,[4] Philip C. Andrews,[3] Anna S. Lok,[2] and M. Bishr Omary[1,2]

[1]Department of Molecular and Integrative Physiology, [2]Department of Internal Medicine, and [3]Department of Biological Chemistry, University of Michigan, Ann Arbor, MI 48109
[4]Division of Gastroenterology, Department of Medicine, Kurume University School of Medicine, Kurume, Fukuoka-ken 830-0011 Japan

Genetic factors impact liver injury susceptibility and disease progression. Prominent histological features of some chronic human liver diseases are hepatocyte ballooning and Mallory-Denk bodies. In mice, these features are induced by 3,5-diethoxycarbonyl-1,4-dihydrocollidine (DDC) in a strain-dependent manner, with the C57BL and C3H strains showing high and low susceptibility, respectively. To identify modifiers of DDC-induced liver injury, we compared C57BL and C3H mice using proteomic, biochemical, and cell biological tools. DDC elevated reactive oxygen species (ROS) and oxidative stress enzymes preferentially in C57BL livers and isolated hepatocytes. C57BL livers and hepatocytes also manifested significant down-regulation, aggregation, and nuclear translocation of glyceraldehyde 3-phosphate dehydrogenase (GAPDH). GAPDH knockdown depleted bioenergetic and antioxidant enzymes and elevated hepatocyte ROS, whereas GAPDH overexpression decreased hepatocyte ROS. On the other hand, C3H livers had higher expression and activity of the energy-generating nucleoside-diphosphate kinase (NDPK), and knockdown of hepatocyte NDPK augmented DDC-induced ROS formation. Consistent with these findings, cirrhotic, but not normal, human livers contained GAPDH aggregates and NDPK complexes. We propose that GAPDH and NDPK are genetic modifiers of murine DDC-induced liver injury and potentially human liver disease.

Introduction

Race and ethnicity have been shown to be important factors in the development and progression of liver diseases for reasons that go beyond socioeconomic status (Nguyen and Thuluvath, 2008). Understanding the biological basis for susceptibility to liver diseases may provide insights into novel therapeutic strategies for their prevention and treatment. Alcoholic liver disease (ALD) and nonalcoholic steatohepatitis (NASH), which represent a significant societal burden, also have a strong genetic component (Anstee et al., 2011). Hepatocyte ballooning and protein aggregation in the form of Mallory-Denk bodies (MDBs) are common characteristics of the liver injury phenotype and correlate with worse outcomes in patients with ALD and NASH (Cortez-Pinto et al., 2003; Gramlich et al., 2004). However, MDB accumulation is not observed in all patients with the same liver disease (Gerber et al., 1973; Fleming and McGee, 1984), and MDBs may be more prevalent in Hispanics in comparison with other groups (Mohanty et al., 2009; Rakoski et al., 2011).

One approach toward understanding the biological basis for these genetic differences in patient populations is to delineate the mechanisms of hepatocyte injury in animal models with varying genetic susceptibility. To that end, we previously found that experimental induction of hepatocyte ballooning and MDBs in mouse livers by using an established model of chronic administration of 3,5-diethoxycarbonyl-1,4-dihydrocollidine (DDC; Yokoo et al., 1982; Zatloukal et al., 2007) manifests in a highly strain-dependent manner (Hanada et al., 2008). Comparison of five inbred mouse strains (Beck et al., 2000) with

Correspondence to Natasha T. Snider:nsnider@umich.edu

Abbreviations used in this paper: ALD, alcoholic liver disease; DDC, 3,5-diethoxycarbonyl-1,4-dihydrocollidine; DIGE, differential in-gel electrophoresis; FAH, fumarylacetoacetate hydrolase; GAPDH, glyceraldehyde 3-phosphate dehydrogenase; MDB, Mallory-Denk body; MS, mass spectrometry; NASH, nonalcoholic steatohepatitis; NDPK, nucleoside-diphosphate kinase; ROS, reactive oxygen species.

The Rockefeller University Press $30.00
J. Cell Biol. Vol. 195 No. 2 217–229
www.jcb.org/cgi/doi/10.1083/jcb.201102142

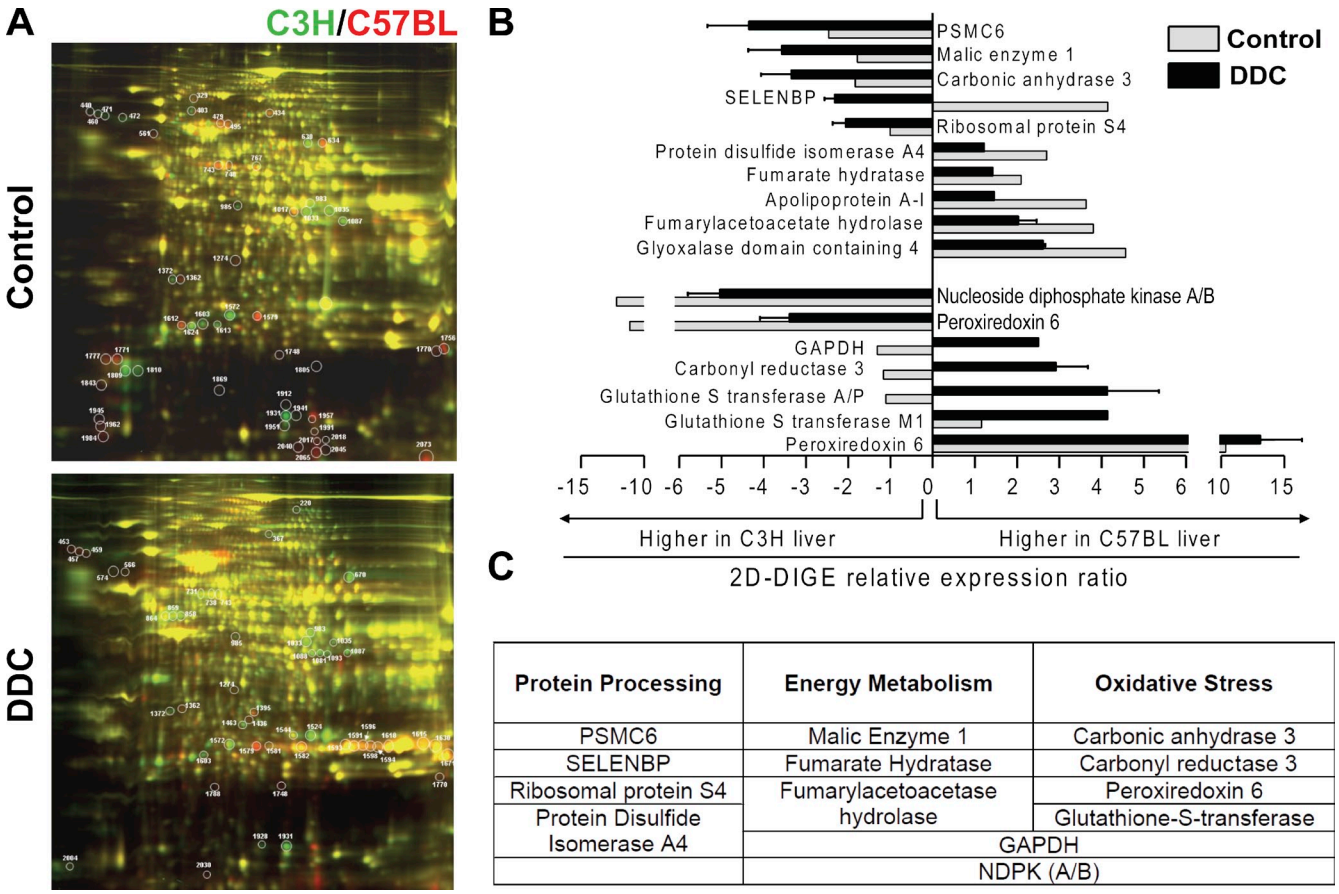

Protein Processing	Energy Metabolism	Oxidative Stress
PSMC6	Malic Enzyme 1	Carbonic anhydrase 3
SELENBP	Fumarate Hydratase	Carbonyl reductase 3
Ribosomal protein S4	Fumarylacetoacetase hydrolase	Peroxiredoxin 6
Protein Disulfide Isomerase A4		Glutathione-S-transferase
	GAPDH	
	NDPK (A/B)	

Figure 1. **Proteomic comparison of C3H and C57BL mouse livers before and after DDC treatment by 2D DIGE analysis and classification of differentially expressed proteins into function-based groups.** (A) Liver homogenates were prepared from untreated mice (Control) or mice fed a DDC-containing diet for 3 mo. The liver proteins from the C3H and C57BL mice were labeled with the fluorescent dyes Cy3 (green) and Cy5 (red), respectively. The circled spots indicate differentially expressed proteins that were selected for identification by MS. (B) From an initial analysis of 80 selected gel spots, proteins that were identified as having significant expression differences (ratio greater than two) between the two mouse strains under basal conditions or after DDC treatment are shown. Note that PRDX6 is represented twice, reflecting the acidic and basic forms of the protein. (C) The proteins shown in B were classified into three groups based on their known functional properties.

distinct genealogies (FVB/N, C3H/He, Balb/cAnN, C57BL/6, and 129X1/Sv) for their susceptibility to DDC-induced hepatocyte ballooning and MDBs identified the C57BL/6 and C3H/He strains (hereafter referred to as C57BL and C3H) as being most and least susceptible, respectively (Hanada et al., 2008). The molecular constituents of MDBs, which mainly include cytoskeletal and stress proteins, indicate that they share common characteristics with nonepithelial cell inclusions of inherited and age-related brain and muscular diseases (Muchowski and Wacker, 2005; Askanas et al., 2009; Goldfarb and Dalakas, 2009; Liem and Messing, 2009). Therefore, elucidating the factors that likely underlie MDB formation in hepatocytes may also provide insights into neuro- and myodegenerative disorders involving protein aggregation.

In the current study, we performed 2D differential in-gel electrophoresis (DIGE) and mass spectrometric proteomic comparison of healthy and DDC-injured livers of MDB-susceptible (C57BL) and MDB-resistant (C3H) mice. We then evaluated the differentially expressed proteins and their corresponding signaling pathways in isolated hepatocytes and in normal and diseased mouse and human livers. Our findings indicate that elevated oxidative stress impairs energy metabolism by promoting glyceraldehyde 3-phosphate dehydrogenase (GAPDH) downregulation and redistribution from a soluble cytoplasmic form into insoluble aggregates residing in the cytoplasm and nucleus. Furthermore, we show that GAPDH is an upstream regulator of several antioxidant and energy metabolism enzymes, including nucleoside-diphosphate kinase (NDPK). Therefore, inadequate supply of energy equivalents likely diminishes the cell's capacity to properly fold and degrade proteins, likely leading to hepatocyte injury and protein aggregation in the form of MDBs.

Results

Proteomic comparison of C3H and C57BL mouse livers before and after DDC treatment

A 2D DIGE analysis was conducted to compare the liver proteome of C3H (MDB resistant) and C57BL (MDB susceptible) mice. This approach yielded a large number of differentially expressed proteins in untreated and DDC-treated mice from the two strains (Fig. 1 A). The circled green- and red-colored spots (Fig. 1 A) were subsequently subjected to tandem mass spectrometry (MS/MS) for protein identification and determination

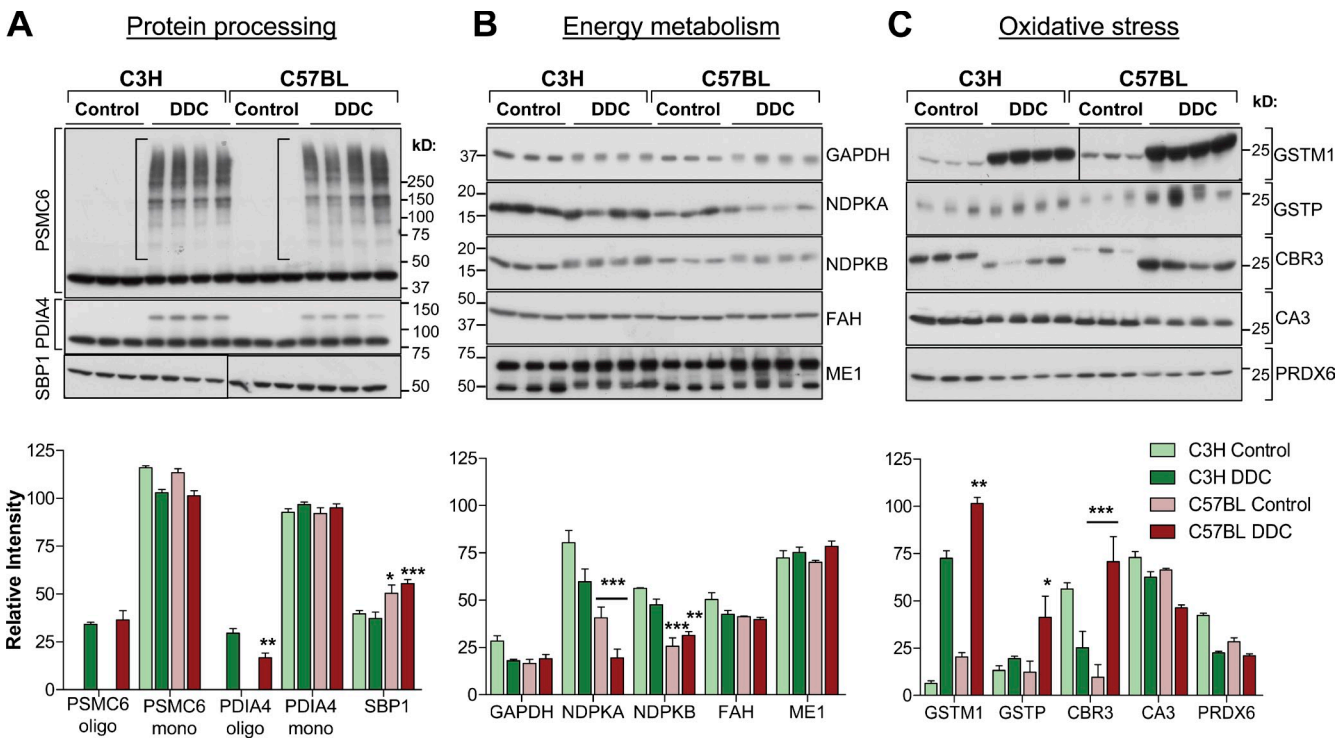

Figure 2. **Strain-specific and DDC-induced changes in the expression of regulators of protein processing, energy metabolism, and oxidative stress.** (A–C, top panels) Equal amounts of total liver protein from three untreated and four DDC-fed C3H or C57BL mice were resolved on SDS-PAGE gels and immunoblotted with antibodies to the indicated proteins. Blots separated by solid lines indicate nonconsecutive lanes of the same equally exposed membrane. The expression of some proteins (PDIA4, FAH, and ME1) was relatively unaffected across groups, and they serve as loading controls. (bottom panels) Relative band intensity values were plotted for each protein in the three different groups. ME1, malic enzyme 1; mono, monomer; oligo, oligomer. *, $P < 0.05$; **, $P < 0.01$; ***, $P < 0.001$ using a two-way analysis of variance. Each tested group included three to four mice. Results are represented as the mean and the SD.

of the relative expression ratios between the two strains. Of 80 targets whose identity was characterized by MS/MS, those that had the highest expression difference either before of after DDC treatment were selected for further characterization (Fig. 1 B). Function-based classification of the identified proteins resulted in three major functional categories: (1) protein processing, (2) energy metabolism, and (3) oxidative stress, with some overlap between the latter two (Fig. 1 C).

Biochemical evidence of strain-specific and DDC-related changes in the expression of regulators of protein processing

The proteomic data were subsequently subjected to further biochemical validation (Fig. 2). The expression of proteasome 26S ATPase subunit 6 (PSMC6), which catalyzes the ATP-dependent 26S proteasomal degradation of ubiquitinated proteins (Smith et al., 2006), was significantly different between control and DDC-treated livers with respect to the existence of oligomeric PSMC6 complexes (Fig. 2 A, brackets), which is consistent with proteasomal impairments in this model (Harada et al., 2008), although there were no significant strain differences. At the mRNA level, PSMC6 was higher in the C3H strain under control conditions and elevated upon DDC treatment, whereas it was diminished upon DDC treatment in the C57BL livers (Table S1). The expression levels of monomeric protein disulfide isomerase A4 (PDIA4), which catalyzes oxidative protein folding in the ER (Gruber et al., 2006), were identical between the two strains. In C57BL livers, there were slightly higher levels of selenium-binding protein 1 (SBP1; Fig. 2 A), which has been implicated in intra-Golgi transport and in selenium-dependent ubiquitination- and deubiquitination-mediated protein degradation pathways (Porat et al., 2000; Jeong et al., 2009). This was in contrast to the mRNA levels, which showed the opposite patterns (i.e., higher SBP1 mRNA in C3H livers) both before and after DDC treatment. The discordance between the protein and mRNA levels may reflect extensive posttranslational regulation of SBP1 and/or antibody reactivity with other SBP isoforms such as SBP2 (Lanfear et al., 1993). Although there were no major strain differences with regards to the total expression levels of PSMC6, PDIA4, and SBP1, the requirement of energy and reducing equivalents for their proper function suggests that differences may exist at the functional level. Therefore, we next examined the expression of energy metabolism regulators.

Biochemical evidence of strain-specific and DDC-related changes in the expression of energy metabolism enzymes

Major differences in the expression of NDPK-A and -B isoforms were observed between the two strains, with a significantly lower expression in C57BL livers under both control and DDC-treatment conditions (Fig. 2 B). The NDPK protein differences

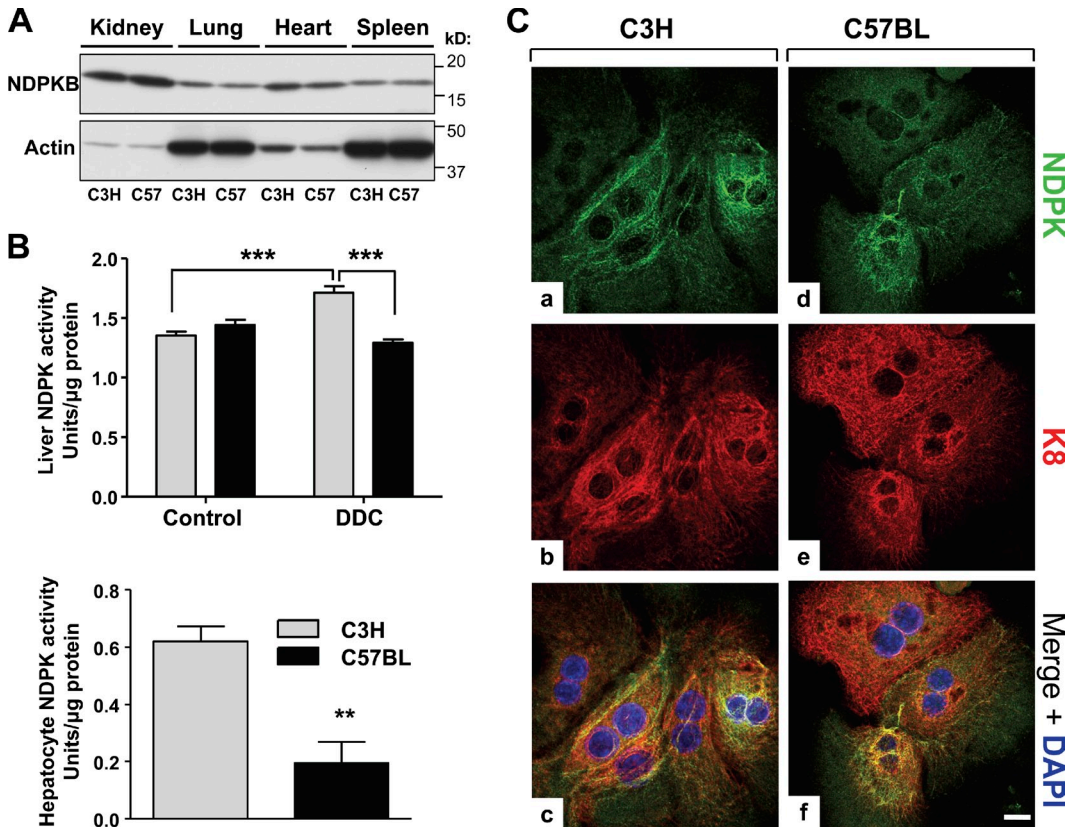

Figure 3. **Hepatic differences in the expression, activity, and distribution of the cytoplasmic enzyme NDPK.** (A) Relative expression level of NDPK-B in extrahepatic organs from C3H and C57BL mice. The actin blot serves as a loading control. (B) Total NDPK activity in C3H and C57BL mouse livers under basal conditions and after DDC treatment (top) and in untreated isolated hepatocytes (bottom). **, $P < 0.01$ using an unpaired *t* test; ***, $P < 0.001$ using a two-way analysis of variance. Each tested group included three to four mice, and samples were analyzed in triplicates. Results are represented as the mean and the SD. (C) Primary cultured hepatocytes from C3H (panels a–c) and C57BL (panels d–f) mice were triple immunostained for NDPK-B and K8 and were then mounted in the presence of DAPI as described in Materials and methods. Bar, 10 µm.

were not reflected at the mRNA level (Table S1), implying a posttranslational control of NDPK expression. NDPK activity is important for the synthesis of non–ATP nucleoside triphosphates (i.e., CTP, GTP, and UTP) via the transfer of a phosphate group from ATP (Boissan et al., 2009). NDPK also plays a role in the protection from oxidative stress–induced damage (Arnaud-Dabernat et al., 2004; Lee et al., 2009). The striking strain differences in liver NDPK expression (Fig. 2 B) were liver specific, as kidney, lung, heart, and spleen NDPK-B levels were similar between the two strains (Fig. 3 A). Further, total NDPK activity was significantly higher in C3H livers after DDC treatment in comparison with control C3H and DDC-treated C57BL livers (Fig. 3 B, top). The differences were more dramatic when assessing total NDPK activity in isolated C57BL hepatocytes, which was threefold lower compared with C3H hepatocytes (Fig. 3 B, bottom). NDPK exhibited a cytoplasmic filamentous organization and partial colocalization with keratin filaments in the hepatocytes (Fig. 3 C), although coimmunoprecipitation experiments did not show a direct interaction between the two (not depicted).

In addition to NDPK, the protein expression of the glycolytic enzyme GAPDH was higher in the control C3H mice than all other groups (Fig. 2 B). At the mRNA level, GAPDH was approximately twofold higher at basal conditions in C3H livers versus C57BL and exhibited an induction in C3H and suppression in C57BL livers after DDC treatment (Table S1). In addition to its traditional role in glycolysis and ATP generation, GAPDH performs numerous other functions, including redox sensing, in which oxidative stress–induced aggregation and nuclear translocation of GAPDH mediate cell death (Nakajima et al., 2009). Given the multiple roles of the housekeeping enzymes NDPK and GAPDH across energy metabolism and oxidative stress responses, these data highlight a potential cross-regulation between these two pathways in DDC-induced liver injury.

Strain-specific and DDC-related changes in the expression of oxidative stress–related enzymes and reactive oxygen species (ROS)

In both mouse strains, DDC significantly induced the expression of the antioxidant GSTs Mu and Pi (GSTM and GSTP) enzymes, which are critical for the detoxification of xenobiotics (Fig. 2 C; Whalen and Boyer, 1998). These data, in combination with previous results showing mouse sex differences in the handling of oxidative stress (Hanada et al., 2010), support a central role for oxidative stress in DDC-induced liver injury. Other antioxidant enzymes, including carbonic anhydrase 3 (CA3) and peroxiredoxin 6 (PRDX6), which are induced by oxidative stress and protect against hydrogen peroxide–induced damage (Räisänen et al., 1999; Wood et al., 2003; Chowdhury et al., 2009), had lower mRNA (Table S1) and protein (Fig. 2 C) expression in C57BL

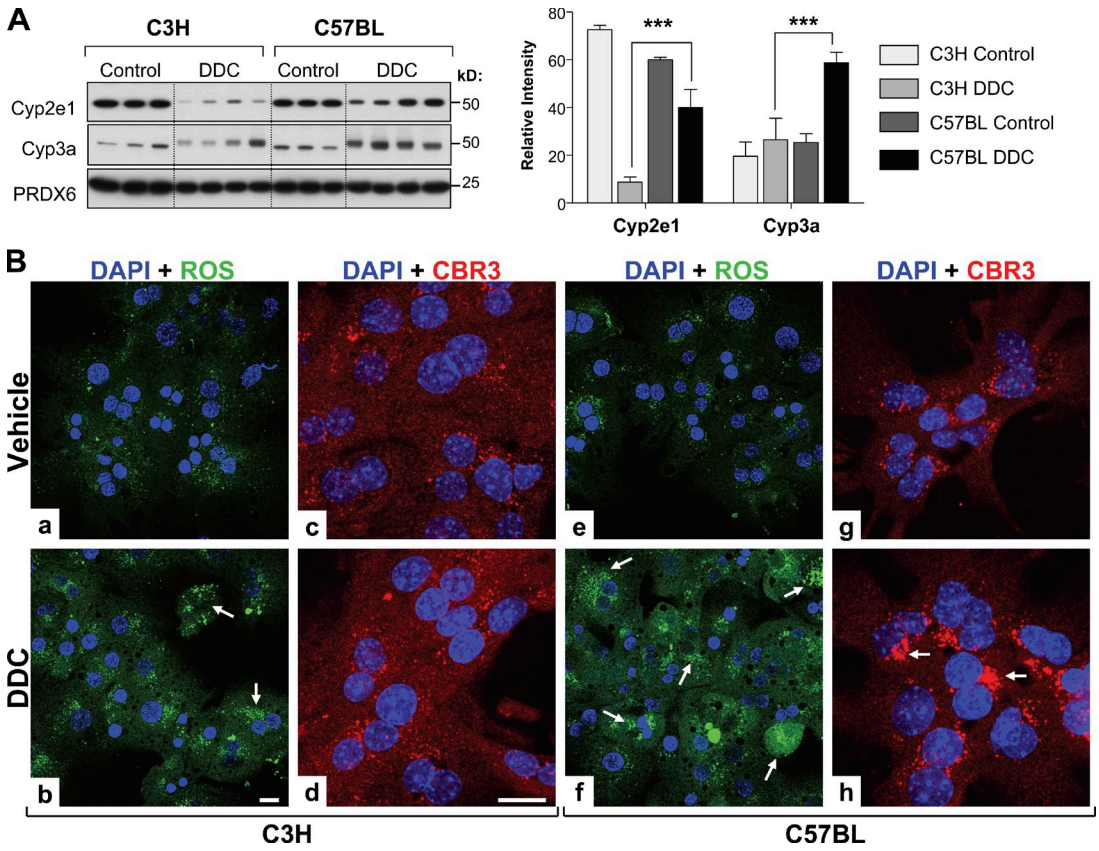

Figure 4. **Strain-specific differences in oxidative stress–related enzymes and ROS.** (A, left) Equal amounts of total liver protein from three untreated and four DDC-fed C3H and C57BL mice were resolved by SDS-PAGE and immunoblotted with antibodies to Cyp2e1 or Cyp3a. The PRDX6 blot serves as a loading control. (right) Relative band intensity values of the blots were plotted for each strain/treatment group. ***, $P < 0.001$ using a two-way analysis of variance. Each tested group included three to four mice. Results are represented as the mean and the SD. (B) Isolated primary hepatocytes from C3H (panels a–d) and C57BL (panels e–h) mice were cultured in the presence of DDC or vehicle (0.1% DMSO), loaded with the ROS indicator CM-H_2DCFDA (panels a, b, e, and f) or immunostained for CBR3 (panels c, d, g, and h), and then mounted in the presence of DAPI as described in Materials and methods. Qualitative assessment of ROS levels (arrows in b and f) is based on CM-H_2DCFDA fluorescence (green). CBR3 appears as perinuclear particulates (arrows in panel h). Bars, 20 µm.

livers. Furthermore, C3H and C57BL livers differed significantly with respect to the presence of charged isoforms of PRDX6 (Fig. S1 A), which is consistent with the known functional regulation of PRDX6 by phosphorylation (Wu et al., 2009) and carbonylation (Wong et al., 2008). Of note, a major strain difference was observed in the expression of carbonyl reductase 3 (CBR3; Fig. 2 C), which catalyzes the reduction of carbonyls and is known to be regulated by the antioxidant nuclear factor erythroid 2–related factor 2 (Nrf2) signaling pathway (Ebert et al., 2010; Klaassen and Reisman, 2010). A significant (eightfold) induction in liver CBR3 expression was noted only in the C57BL but not the C3H mouse livers. Consistent with the lack of CBR3 induction, C3H livers exhibited increased protein carbonylation after DDC treatment, which was not the case in the C57BL livers (Fig. S1 B).

Next, we examined the expression of prooxidant liver enzymes and ROS generation. The expression of Cyp2e1, a known ROS-generating enzyme implicated in the pathogenesis of ALD (Cederbaum et al., 2009), and Cyp3a, the enzyme responsible for mouse liver DDC metabolism (Hanada et al., 2010), was significantly different between the two strains after DDC treatment (Fig. 4 A). Specifically, Cyp2e1 expression was down-regulated by 90% in the C3H and by only 30% in the C57BL livers, resulting in a fivefold higher relative Cyp2e1 expression in C57BL compared with C3H livers after DDC treatment. The apparent decrease in Cyp2e1 protein was not a result of the contribution of bile ductular epithelium to total liver protein, as induction of K19 (ductal marker) was similar between the two strains (Fig. S2 A), which is in agreement with previous findings (Hanada et al., 2008). Cyp2e1 mRNA levels also decreased in both strains (Fig. S2 B). In C57BL but not C3H livers, there was a marked Cyp3a induction (Fig. 4 A), which we have previously shown to correlate with the propensity of male mice to form more MDBs compared with female mice (Hanada et al., 2010). The differences in ROS-generating cytochromes P450 (CYPs) and GST induction suggested possible glutathione depletion in the C57BL livers. However, measurement of the total and oxidized glutathione levels between the two strains did not reveal major differences (Fig. S2 C).

Next, we examined the intracellular ROS levels ex vivo in cultured hepatocytes using the probe CM-H_2DCFDA (Eruslanov and Kusmartsev, 2010). As shown in Fig. 4 B (panels a, b, e, and f), DDC triggered a dramatic and more robust increase in ROS levels in C57BL hepatocytes in comparison with C3H hepatocytes. The induction of ROS correlated proportionately with increased CBR3 immune staining in DDC-treated C57BL

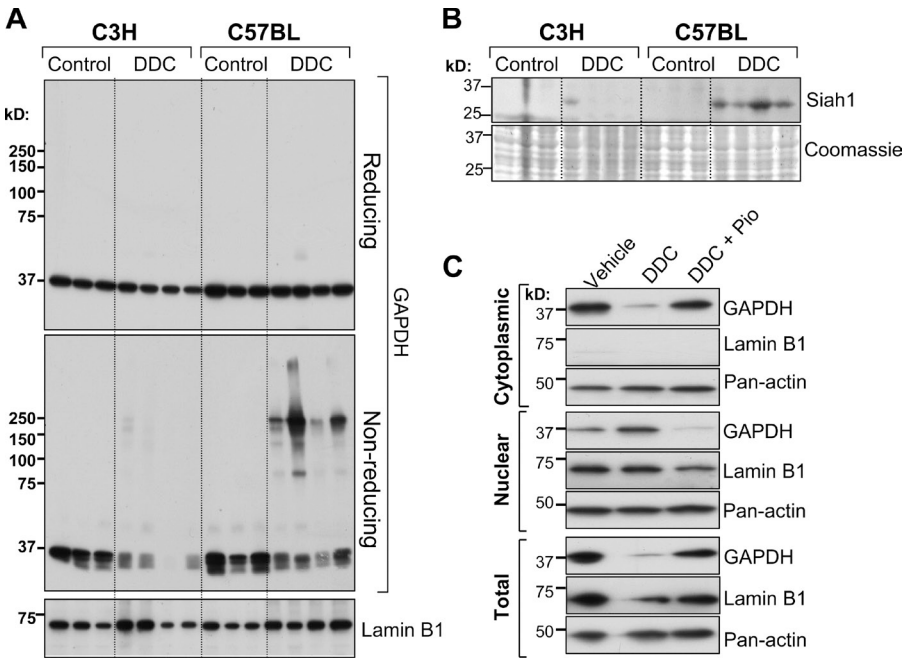

Figure 5. **Differences in GAPDH aggregation and Siah1 levels in C57BL and C3H mouse livers and effect of pioglitazone on DDC-modulated GAPDH nuclear localization in C57BL hepatocytes.** (A) Nuclear fractions were prepared from C3H and C57BL mouse livers (livers from control diet [*n* = 3] or DDC-fed mice [*n* = 4]; groups are separated by dotted lines) and analyzed on the same gel by SDS-PAGE followed by immunoblotting for GAPDH under reducing or nonreducing conditions. Lamin B1 was used as a loading control. Significant levels of high molecular weight nuclear GAPDH aggregates were detected only in C57BL livers after DDC exposure. (B) C57BL livers (three independent control livers/strain and four separate livers from DDC-fed mice) express significantly higher levels of Siah1 protein after DDC treatment. Coomassie stain serves as loading control. (C) Biochemical analysis on total, cytoplasmic, and nuclei-enriched fractions from C57BL hepatocytes. The hepatocytes were cultured in the presence of vehicle (DMSO), 100 µM DDC, or 3 µM pioglitazone (Pio) plus DDC for 48 h. Detergent lysates were then prepared and blotted with antibodies to GAPDH, lamin B1 (nuclear marker), β-tubulin (cytoplasmic marker), and pan-actin (loading control).

hepatocytes (Fig. 4 B, panels c, g, d, and h), which is consistent with the immunoblotting data (Fig. 2 C) and the dramatic increase in CBR3 mRNA levels (Table S1). These findings indicate that there is elevated oxidative stress in C57BL hepatocytes, triggering activation of antioxidant responses.

Presence of nuclear GAPDH aggregates in DDC-treated C57BL mouse livers and isolated hepatocytes

Given the major oxidative and metabolic differences between the MDB-resistant and MDB-susceptible mice, we focused our attention on the status of GAPDH as a potential common regulator of these pathways. Prior studies showed that oxidative stress induces extensive GAPDH modification and aggregation, which leads to its inactivation and compromised glycolysis (Nakajima et al., 2007, 2009; Tristan et al., 2011). Furthermore, upon nitrosylation (Hara et al., 2005) and association with the E3 ubiquitin ligase Siah1, GAPDH translocates to the nucleus and regulates autophagy induction (Colell et al., 2007), nuclear protein nitrosylation (Kornberg et al., 2010), and apoptotic cell death (Hara et al., 2005). To determine whether GAPDH aggregation and nuclear translocation occur in vivo after DDC treatment, we analyzed the nuclear fractions of livers from both mouse strains and found that total and aggregated nuclear GAPDH were significantly more abundant in C57BL livers (Fig. 5 A). Of note, the GAPDH aggregates were observed only when analyzed under nonreducing conditions, which is consistent with their intermolecular disulfide-bonded nature. The increased C57BL nuclear GAPDH after DDC exposure (Fig. 5 A) correlated with significantly higher levels of Siah1 protein (which is involved in GAPDH nuclear translocation) in C57BL livers after DDC treatment (Fig. 5 B). Biochemical analysis of C57BL hepatocyte total, cytoplasmic, and nuclei-enriched fractions showed that DDC caused a significant reduction in the total and cytoplasmic levels of GAPDH to 12 and 14%, respectively, as compared with vehicle levels (Fig. 5 C). In contrast, there was an increase of 215% in the nuclear levels of GAPDH after exposure to DDC. Of note, cotreatment with the insulin sensitizer pioglitazone almost completely reversed the total and cytoplasmic DDC-induced GAPDH depletion to 80% of vehicle and decreased the nuclear accumulation to 23% of vehicle (Fig. 5 C). Collectively, these data demonstrate a pharmacologically amenable role for GAPDH in hepatocellular injury.

We also investigated the presence of GAPDH in the detergent-insoluble fraction of isolated hepatocytes and compared it with actin in the same fractions. C57BL, but not C3H, hepatocytes contained significant amounts of insoluble GAPDH (Fig. 6 A). Furthermore, immunofluorescence staining showed that DDC induced the nuclear translocation of GAPDH in C3H hepatocytes (Fig. 6 B, panels a, b, e, and f). In stark contrast, GAPDH is already present in the nuclei of C57BL hepatocytes under basal conditions (Fig. 6 B, panels c and d) but undergoes aggregation upon exposure to DDC (Fig. 6 B, panels g and h).

Strain-dependent effect of DDC on ex vivo hepatocyte expression and activity of energy metabolism and antioxidant enzymes

We performed additional ex vivo experiments of isolated hepatocytes from C3H and C57BL mice to further explore the effects that were seen after DDC treatment in vivo. Similar to the in vivo findings (Fig. 2), ex vivo analysis showed that NDPK-B, CA3, and PRDX6 expression decreased after DDC treatment, whereas PDIA4 levels remained unchanged (Fig. 7 A; quantification is shown in Fig. S3 A). There was also a significant dose-dependent decrease in GAPDH and the tyrosine catabolism enzyme fumarylacetoacetate hydrolase (FAH) expression upon DDC treatment (Fig. 7 A), indicating a significant impairment in metabolic activity. These changes were more striking in C57BL hepatocytes, particularly in the case of NDPK-B.

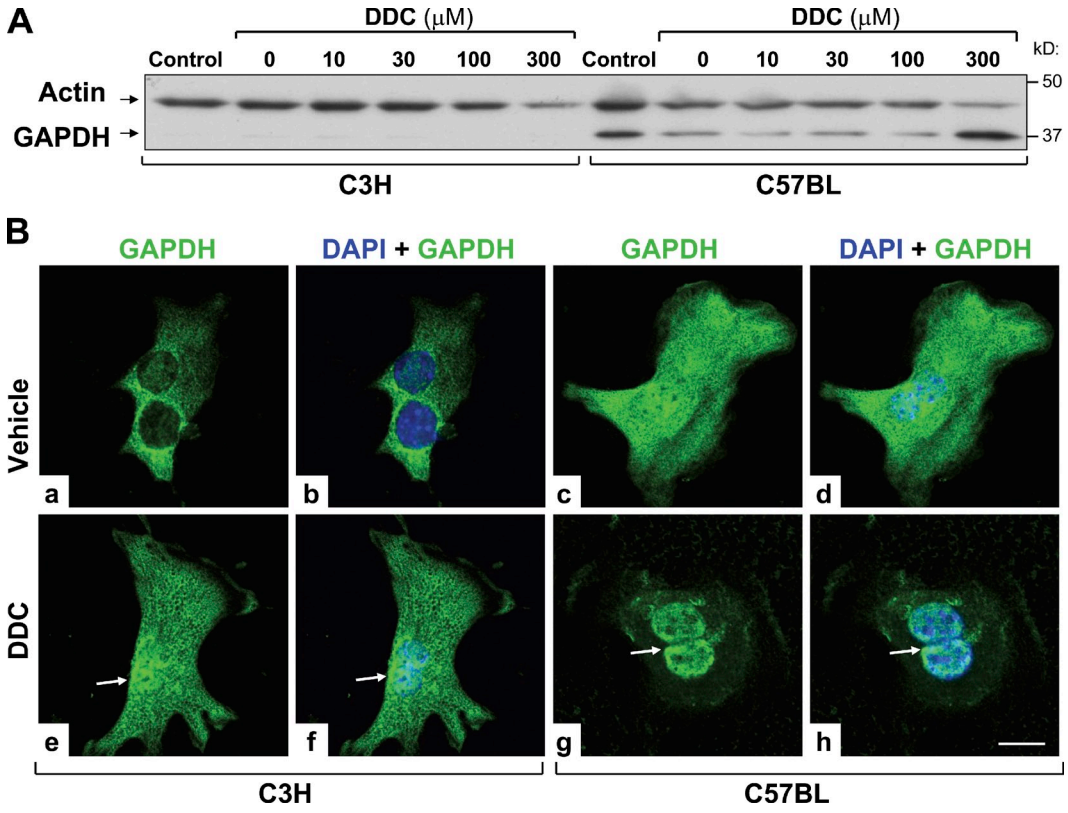

Figure 6. **Presence of detergent-insoluble and nuclear GAPDH in C57BL hepatocytes.** (A) Hepatocytes from C57BL and C3H mice were cultured in presence of the indicated concentrations of DDC or 0.1% DMSO vehicle (0) or in the absence of DDC/DMSO (Control). Detergent-insoluble equal fractions were prepared and then blotted with antibodies to actin (loading control) and GAPDH. (B) Immunofluorescence-based localization of GAPDH in vehicle (DMSO; panels a–d) or DDC-treated hepatocytes (panels e–h) that were also double stained with DAPI (nuclear staining). Note that after DDC treatment, GAPDH translocates to the nucleus in C3H hepatocytes (arrows in panels e and f) and appears to aggregate in the perinuclear region of C57BL hepatocytes (arrows in panels g and h). Bar, 20 μm.

DMSO vehicle alone strongly decreased GAPDH, NDPK-B, and CA3 levels in C57BL hepatocytes (Fig. 7 A). The mechanism behind the DMSO effect is unclear; however, DMSO is known to exert control over the expression of several nuclear transcription factors (Su and Waxman, 2004), which may have contributed to its effects observed herein. DDC treatment augmented the expression of Cyp2e1 in both C3H and C57BL hepatocytes (Fig. 7 A).

GAPDH is an upstream regulator of metabolic and antioxidant enzymes and ROS formation in hepatocytes

We tested whether GAPDH is an upstream regulator of the proteins detected in our proteomic analysis (Figs. 1 and 2), given the known regulatory functions for GAPDH and the major differences in insoluble and nuclear GAPDH observed herein. As shown in Fig. 7 B (compare the first and second lanes with the fourth and fifth lanes), siRNA-mediated knockdown of GAPDH in isolated C57BL hepatocytes caused a significant down-regulation in the expression of NDPK-B (as well as NDPK-A; not depicted), FAH, CA3, and PRDX6 but had no effect on the expression of PDIA4 or Cyp2e1 when compared with control siRNA–transfected hepatocytes (quantification is shown in Fig. S3 B). Notably, the knockdown of GAPDH mimicked the effects of DDC treatment, thereby implicating GAPDH as an upstream regulator of the metabolic and antioxidant DDC-induced responses in hepatocytes. Consistent with this, GAPDH knockdown and overexpression increased 2.2-fold and decreased 10-fold, respectively, the generation of ROS in DDC-treated C57BL hepatocytes (Fig. 7, C–E).

DDC-induced ROS formation in C3H and C57BL hepatocytes is augmented by GAPDH and NDPK knockdown

We compared ROS formation in DDC-treated C3H and C57BL hepatocytes upon NDPK and GAPDH knockdown. The remaining protein levels were 1.5–5% for GAPDH and 23–55% for NDPK after the treatment with the specific siRNA (Fig. 8 A). NDPK knockdown also caused a decrease in GAPDH levels to 68% in C3H and 41% in C57BL hepatocytes, indicating a coregulation between GAPDH and NDPK, which may be a result of changes in the cellular availability of nucleoside triphosphates. For example, a decrease in NDPK, which uses ATP to generate non–ATP nucleoside triphosphates (Boissan et al., 2009), could result in an increase in cytoplasmic ATP, which is an allosteric inhibitor of rate-limiting enzymes in glycolysis and thus may affect GAPDH levels (Berg et al., 2002). The representative images in Fig. 8 B show elevated ROS levels after GAPDH or NDPK knockdown in DDC-treated C3H and C57BL hepatocytes. Quantification of the

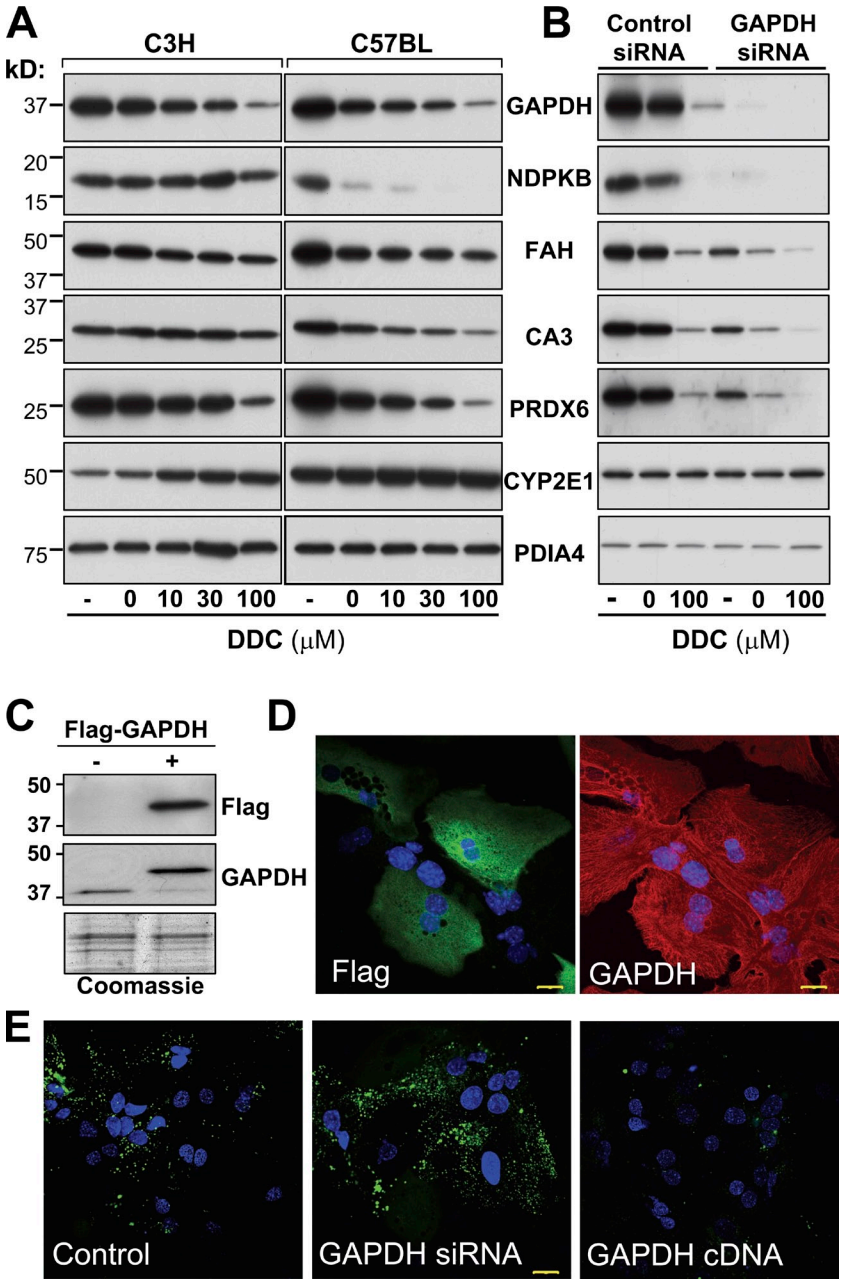

Figure 7. **DDC-induced ROS formation is associated with a depletion of energy metabolism and antioxidant enzymes and is regulated by GAPDH.** (A) Hepatocytes from C3H and C57BL mice were left untreated (−) or treated with either 0.1% DMSO vehicle (0) or the indicated concentrations of DDC for 48 h. Equal protein amounts (NP-40 lysates) were analyzed for expression of the indicated proteins. Samples from each strain were analyzed on separate gels. PDIA4 levels were unaltered (loading control). (B) C57BL hepatocytes were transfected with Control or GAPDH siRNA for 24 h and were then cultured for an additional 24 h in the presence of 0.025% DMSO vehicle (0) or 100 µM DDC or were left untreated (−). The NP-40 cell lysates were analyzed for the expression of the various proteins indicated. (C) Overexpression of Flag-tagged mouse GAPDH in isolated hepatocytes. NP-40 lysates were analyzed for expression of Flag-tagged GAPDH and total GAPDH. The Coomassie stain is included as a loading control. (D) Flag-GAPDH expression in C57BL hepatocytes, as determined by immunostaining with a mouse anti-Flag antibody (representing overexpressed GAPDH; green) and a rabbit anti-GAPDH antibody (representing total GAPDH; red). (E) C57BL hepatocytes were mock transfected (Control) or transfected with GAPDH siRNA or Flag-GAPDH mouse cDNA for 24 h and were then treated with 100 µM DDC for an additional 24 h. Representative images of ROS signal (green) with DAPI nuclear counterstain (blue) are shown. ROS levels (quantified as described in Materials and methods) exhibited a 2.2-fold increase after GAPDH knockdown and a 10-fold decrease after GAPDH overexpression relative to control. Bars, 20 µm.

data from three independent images of each treatment group revealed statistically significant increases in ROS levels in C3H and C57BL hepatocytes upon GAPDH and NDPK knockdown (Fig. 8 C).

GAPDH aggregates and NDPK complexes are present in cirrhotic but not normal human livers

To examine the potential clinical relevance of our findings, we compared the presence of cytoplasmic and nuclear GAPDH aggregates in livers from alcoholic cirrhosis patients with normal control livers. Notably, the diseased but not normal human livers contained cytoplasmic and nuclear GAPDH aggregates (Fig. 9 A). Although there were no significant differences in monomeric NDPK-B protein between normal and diseased livers, the latter contained significant levels of higher molecular weight NDPK-B–containing species (Fig. 9 B). Future identification of the components of these complexes may yield additional mechanistic insight into a potential role of this enzyme in liver disease. Collectively, our findings in the genetically susceptible mouse model of MDB formation may extrapolate to human ALD with respect to GAPDH and NDPK function.

Discussion

In the present study, we tested the hypothesis that genetic factors critically modulate susceptibility to hepatocyte injury in a mouse MDB model. We began with a global approach using 2D DIGE comparison of the basal protein expression levels and DDC-induced changes in livers of C3H (MDB resistant) and

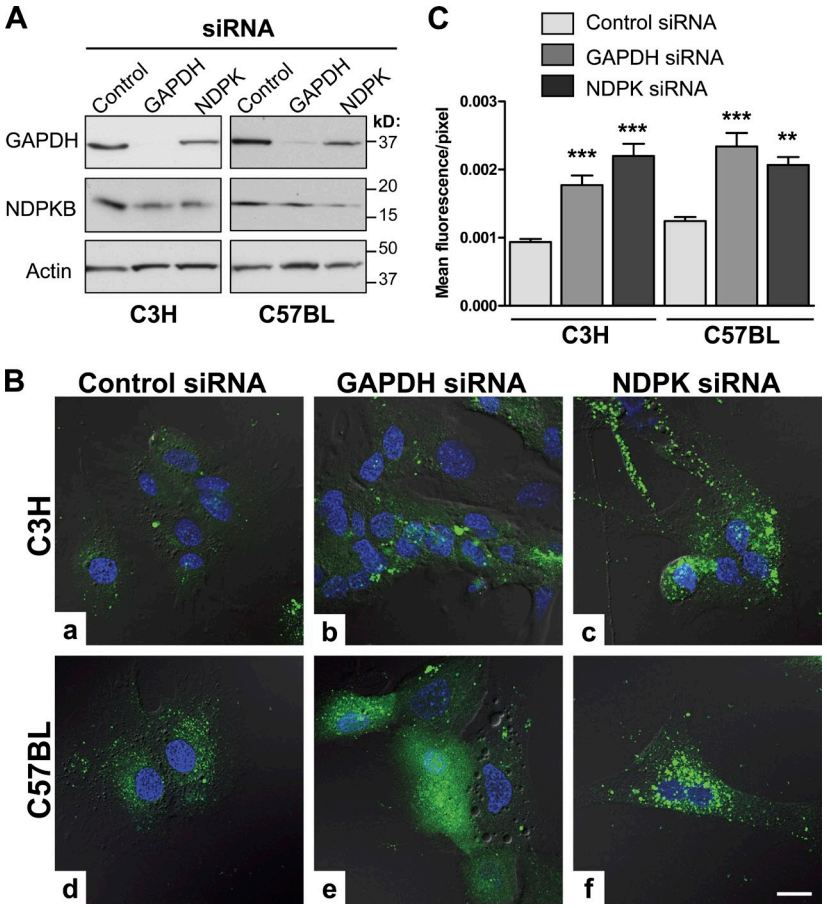

Figure 8. **DDC-induced ROS formation in C3H and C57BL hepatocytes is augmented by GAPDH and NDPK knockdown.** (A) Biochemical analysis of protein expression of GAPDH, NDPK-B, and actin (loading control) 24 h after transfection of the isolated primary hepatocytes with the indicated siRNA. (B) Primary hepatocytes were transfected with the indicated siRNA for 24 h followed by the addition of 100 µM DDC for an additional 24 h. Representative differential interference contrast fluorescence images of ROS levels (green) in C3H and C57BL hepatocytes with DAPI counterstain (blue) are shown. Bar, 20 µm. (C) Quantification of hepatocyte ROS levels upon GAPDH and NDPK knockdown and DDC treatment. **, $P < 0.01$; ***, $P < 0.001$ using a one-way analysis of variance and relative to the respective control group. ROS levels in control-transfected DDC-treated C57BL hepatocytes were significantly higher compared with control-transfected DDC-treated C3H hepatocytes ($P = 0.0009$ using an unpaired *t* test). Results are represented as the mean and the SD ($n = 15$ cells/group), and the data for each tested group are representative of three independent hepatocyte isolations.

C57BL (MDB susceptible) mouse strains. Next, the 2D DIGE-validated findings were used as a starting point to evaluate the status of the most likely candidate proteins and signaling pathways ex vivo in hepatocytes and in vivo in mouse and human livers. Our findings indicate that MDB susceptibility is likely related to basal deficiencies in energy metabolism pathways that are intensified by elevated oxidative stress, ultimately resulting in compromised energy-dependent protein folding/degradation responses (Fig. 10). We propose a central upstream role for GAPDH and its oxidative stress–induced aggregation and nuclear translocation in liver injury–induced hepatocyte inclusion formation. The changes in GAPDH are unlikely to be unique to alcohol-related liver injury because analysis of liver explants from patients with other etiologies of end-stage liver disease also had accumulation of aggregated GAPDH (unpublished data).

Imbalance between oxidative stress load and antioxidant defenses in MDB-susceptible livers

We previously described an important role for microsomal CYP-mediated DDC metabolism and oxidative stress in the gender-dimorphic formation of mouse MDBs (Hanada et al., 2010). Specifically, there is an induction of Cyp3a and sustained high expression of Cyp2e1 in livers of male mice, as contrasted to down-regulation of both of these enzymes in female mice upon chronic DDC exposure (Hanada et al., 2010). This results in increased Cyp3A-mediated DDC metabolism, oxidative stress (e.g., elevated lipid hydroperoxides), and a greater number of MDBs in the male mice (Hanada et al., 2010). The current study lends further support to the role of the microsomal CYPs in the DDC-induced liver injury, as it relates to genetic background.

Contribution by the other proteins that were identified by the 2D DIGE analysis may have also significantly affected the histopathological changes that occur in the C3H and C57BL mice after DDC treatment. For example, exposure of C57BL hepatocytes to DDC in vitro resulted in a more dramatic decrease in the expression of several antioxidant enzymes, including PRDX6 and CA3, when compared with C3H hepatocytes. This suggests that C57BL hepatocytes may experience higher H_2O_2 levels as a result of deficient PRDX6 (Wood et al., 2003) and H_2O_2-induced damage as a result of deficient CA3 (Räisänen et al., 1999). Furthermore, expression of CBR3, a target of the Nrf2 antioxidant system (Ebert et al., 2010; Klaassen and Reisman, 2010), increased dramatically in DDC-treated hepatocytes and livers of C57BL mice in response to the elevated oxidative stress. Consistent with the CBR3 expression differences, total liver protein carbonylation after DDC increased only in the DDC-treated C3H mice. Protein carbonylation plays important roles in cell signaling (Wong et al., 2010). For example, carbonylation of annexin A1 targets it for proteasomal degradation, which in turn promotes cell survival and growth (Wong et al., 2008).

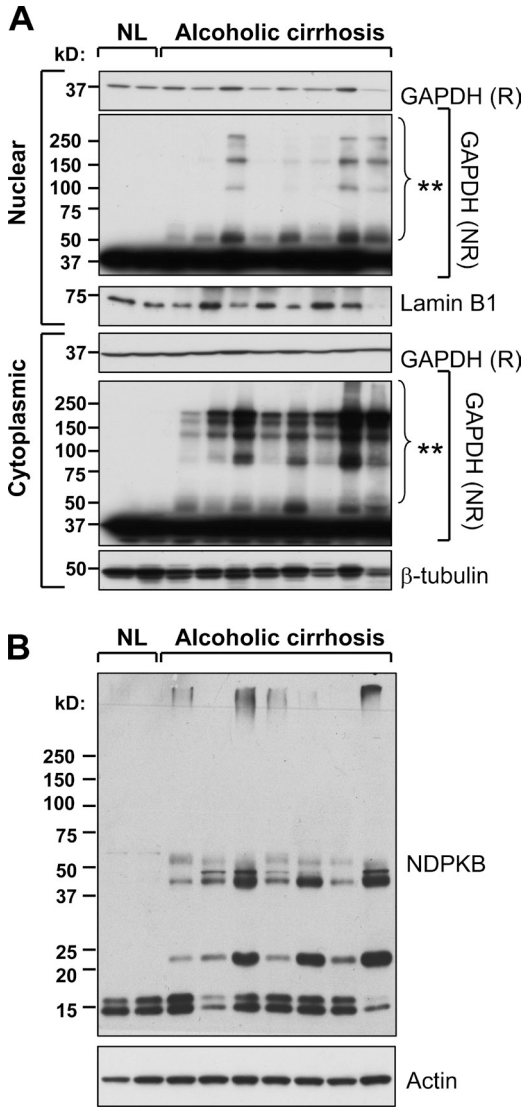

Figure 9. **GAPDH and NDPK-B aggregates are present in nuclei-enriched fractions of human alcoholic cirrhosis livers.** (A) Cytoplasmic and nuclei-enriched fractions from two different normal human livers (NL) and liver explants of eight patients with alcoholic cirrhosis were analyzed by SDS-PAGE followed by blotting for GAPDH (reducing [R] or nonreducing [NR] conditions). Lamin B1 and β-tubulin were used as loading controls for the nuclear and cytoplasmic fractions, respectively. GAPDH aggregates (denoted by asterisks) are present in the diseased but not the normal human livers. (B) Analysis of NDPK-B expression in total liver lysates (under reducing conditions) from the same samples as in A. Higher molecular weight NDPK-B–containing complexes are present in the diseased but not the normal human livers.

MDB susceptibility parallels liver- and hepatocyte-specific differences in NDPK

NDPKs are structurally and functionally conserved enzymes from bacteria to humans, and they regulate intracellular energy pools by catalyzing the transfer of γ-phosphates of a nucleoside triphosphate donor onto a nucleoside diphosphate acceptor and generate CTP, GTP, and UTP (Boissan et al., 2009). Aside from this homeostatic function, NDPKs are known to regulate transcription (Postel et al., 1993) and cell proliferation (Braun et al., 2007) and are a novel therapeutic target for cancer metastasis (Steeg and Theodorescu, 2008). Additionally, NDPKs exert protective effects in the cellular response to oxidative stress, which is attributed to their ability to induce c-myc expression (Arnaud-Dabernat et al., 2004). We demonstrate herein that C57BL livers and hepatocytes exhibit a basal deficiency in NDPK, which is further accelerated by the presence of DDC, and that this contributes to elevated oxidative stress. Furthermore, multiple NDPK-containing protein complexes are present in cirrhotic but not normal human livers, implicating NDPK as a potential target in liver disease.

Stress-induced GAPDH aggregation and nuclear translocation in MDB-susceptible mouse livers

Aside from its role in glycolysis, GAPDH has numerous other important cellular functions, including regulation of cell survival and cell death by way of its aggregation and nuclear translocation (Sen et al., 2008, 2009). Under conditions of oxidative stress, including ethanol-induced stress (Ou et al., 2010), GAPDH translocates to the nucleus or forms amyloid-like aggregates in an irreversible process involving an active site cysteine residue (Nakajima et al., 2009). Neuroprotective agents, such as selegiline and rasagiline, block the ethanol-induced nuclear translocation of GAPDH, thus preventing the cell death–promoting signaling cascade (Ou et al., 2010). This cascade involves the formation of a complex between S-nitrosylated GAPDH with an NLS-containing E3 ubiquitin ligase (Siah1), translocation of the complex to the nucleus, and activation of p300/CREB-binding protein and its target, p53, to induce cell death (Sen et al., 2008).

Our studies in the DDC-injured livers and isolated hepatocytes demonstrate that the redox-sensing role of GAPDH, which has thus far been described in neuronal systems, extends to hepatocytes in the liver. We find that depletion and nuclear accumulation of GAPDH are reversed by pioglitazone, which may provide a potential mechanistic basis for the histological improvements in livers of NASH patients who have been treated with pioglitazone (Promrat et al., 2004; Aithal et al., 2008; Sanyal et al., 2010). For example, in the PIVENS (pioglitazone versus vitamin E versus placebo for the treatment of nondiabetic patients with NASH) trial, a large placebo-controlled clinical trial of pioglitazone in NASH (Sanyal et al., 2010), there were significant improvements in steatosis, lobular inflammation, and hepatocellular ballooning in the pioglitazone compared with the placebo group ($P < 0.001$), which represents a potential clinical context for our findings.

Materials and methods

Antibodies

The antibodies used in the study were to NDPK-A (NME1), NDPK-B (NME2), PSMC6, GAPDH (6C5), CYP3A1, FAH, PDIA4 (ERp72), lamin B1, PRDX6, and Siah1 (Abcam); GSTM1, CBR3, CA3, and ME1 (Santa Cruz Biotechnology, Inc.); panactin and β-tubulin (Thermo Fisher Scientific); SPB1 (MBL International); Troma I (K8) and Troma III (K19; Developmental Studies Hybridoma Bank); mouse anti-DDK (OriGene); and CYP2E1 (a gift from H. Gelboin, National Institutes of Health, Bethesda, MD).

Human and animal liver experiments

The diseased human liver samples were explant tissues from patients who underwent liver transplantation for end-stage liver disease as a result of alcoholic cirrhosis and were used under an approved Human

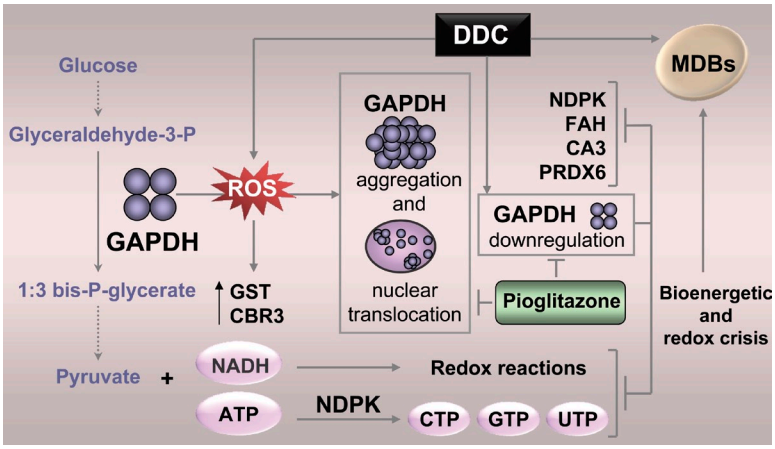

Figure 10. **Compromised energetics and redox cycling contribute to MDB formation in C57BL mice.** DDC causes oxidative stress in vivo, as indicated by the significant induction of liver GST and CBR3 expression, and ex vivo in isolated hepatocytes, as indicated by the accumulation of intracellular ROS. Elevated ROS promotes aggregation and nuclear translocation of GAPDH in the livers of DDC-fed mice and in DDC-treated isolated hepatocytes. Ex vivo DDC treatment of hepatocytes causes a significant down-regulation of GAPDH. Furthermore, GAPDH is a central regulator of energy metabolism and oxidative stress–related enzymes, including NDPK, FAH, CA3, and PRDX6, as GAPDH knockdown leads to significant decreases in the expression of these proteins and mimics the effect of DDC. Therefore, diminished GAPDH expression and function lead to a bioenergetic and redox crisis, compromising energy-dependent protein processing pathways and ultimately leading to MDB formation. The glycolysis-stimulating agent pioglitazone reverses the GAPDH down-regulation and nuclear translocation.

Subjects protocol (Ku et al., 2005). Nondiseased (normal) human liver tissues were obtained from the National Disease Research Interchange. Animal use was approved by and performed in accordance with the University Committee on Use and Care of Animals at the University of Michigan. DDC feeding for 3 mo to induce MDBs was performed as previously described (Hanada et al., 2008). In brief, eight mice per strain were fed a powdered chow diet (Formulab Diet 5008; Dean's Animal Feeds) supplemented with 0.1% DDC wt/wt (Sigma-Aldrich) for 3 mo. Age-matched males (three mice per strain) were kept on a standard mouse diet (Teklad Global Diet 2019; Harlan Laboratories, Inc.) and were used as controls.

2D DIGE and MS-based proteomic comparison of C3H and C57BL livers

2D DIGE was performed as previously described (Marouga et al., 2005). Liver homogenates from untreated and DDC-treated age-matched C3H and C57BL male mice were labeled with the fluorescent dyes Cy3 (green) and Cy5 (red), respectively. The samples were mixed and resolved by 2D gel electrophoresis, and the differentially expressed proteins (indicated by green or red fluorescence) were selected for identification by MS/MS analysis. Approximately 140 spots (circled in Fig. 1 A) were selected for MS-based identification.

Hepatocyte isolation and treatments

Primary hepatocytes from 12–14-wk-old male C3H and C57BL mice were isolated as previously described (Snider et al., 2011). In brief, the mice were anesthetized with 50 mg/kg Nembutal (Lundbeck Inc.), and the liver was perfused (7 ml/min) with 30 ml of solution I (Hank's balanced salt solution containing 0.5 mM EGTA, 5.5 mM glucose, and 1% penicillin-streptomycin) followed by 25 ml of solution II (Hank's balanced salt solution containing 1.5 mM $CaCl_2$, 5.5 mM glucose, 1% penicillin-streptomycin, and 2,000 U of collagenase IV [Worthington Biochemical Corporation]). Upon gentle mechanical dispersion of the liver, the cell suspension was filtered through a 70-µm cell strainer and pelleted (500 rpm for 2 min at 4°C), and the cells were cultured in Williams' medium E containing 10% FBS and 1% penicillin-streptomycin on collagen-coated dishes. The hepatocytes were allowed to attach for 8 h (at 37°C in 5% CO_2) before the addition of siRNA constructs, DDC (in DMSO), DMSO, or DDC plus pioglitazone. For GAPDH and NDPK knockdown, hepatocytes were grown in 6-well plates (biochemical experiments) or 4-well chamber slides (immunofluorescence experiments) and were transfected with either control or GAPDH or NDPK-A + NDPK-B siRNA (Santa Cruz Biotechnology, Inc.) using Lipofectamine RNAiMAX reagent (Invitrogen) with 30 pmol siRNA and 5 µl Lipofectamine (per well on the 6-well plate). The medium was replaced after 6 h, and the cells were incubated for an additional 18 h before the addition of DDC. Transfection of Flag-tagged mouse GAPDH cDNA (OriGene) was performed using Lipofectamine LTX (Invitrogen) according to the manufacturer's instructions. siRNA and DNA-transfected hepatocytes were exposed to 100 µM DDC for 24 h.

Preparation of liver and hepatocyte lysates and immunoblotting

Livers were homogenized in ice-cold NP-40 buffer (150 mM sodium chloride, 1% NP-40, and 50 mM Tris, pH 8.0) supplemented with protease inhibitors. The NP-40 soluble and insoluble fractions were separated by centrifugation at 14,000 rpm for 20 min (at 4°C). Isolated hepatocytes were either lysed in NP-40 buffer or subjected to subcellular fractionation using the NE-PER cytoplasmic/nuclear fractionation kit (Thermo Fisher Scientific) to obtain total, cytoplasmic, and nuclear-enriched fractions. Liver or hepatocyte lysates were resolved on 4–20% gradient SDS-PAGE gels and were then transferred onto polyvinylidene difluoride membranes, which were subsequently blocked and incubated with the designated antibodies.

Extraction of RNA and quantitative real-time PCR

RNeasy kits (QIAGEN) were used to extract the total RNA from the mouse livers. RNA was translated into cDNA using the TaqMan reverse transcription kit (Applied Biosystems). cDNA was then subjected to quantitative real-time PCR (MyiQ real-time PCR detection system; Bio-Rad Laboratories) and was amplified by Brilliant SYBR green master mix using gene-specific primers (Table S2). 18S RNA was amplified as an internal control. Because the amplification efficiencies for the gene of interest and the internal control were approximately equal, the quantification was expressed as a ratio of $2\Delta^{Ct/gene}$ to $2\Delta^{Ct/internal\ control}$, in which ΔCt/gene and ΔCt/internal control represent the difference between the threshold cycle of amplification for the gene of interest and internal control, respectively. Each tested group included three to four mice, and samples were analyzed in triplicates. Results are represented as the mean and the SD.

Immunofluorescence staining and confocal imaging of primary hepatocytes

After methanol fixation (for 10 min at −20°C), the hepatocytes were air dried, and nonspecific binding was blocked by incubation in blocking buffer (PBS with 2.5% wt/vol BSA and 2% goat serum). Primary antibodies to GAPDH and CBR3 in blocking buffer were incubated with the cells for 1 h (at 22°C) followed by three 5-min washes in PBS and then incubation with secondary Alexa Fluor–conjugated antibodies (for 30 min). After rinsing in PBS, cells were mounted with ProLong Gold containing DAPI (Invitrogen), imaged on a laser-scanning confocal microscope (FluoView 500; Olympus) with a 60× oil immersion (1.4 NA) objective, and magnified with FluoView software (version 5.0; Olympus). DAPI, Alexa Fluor 488, and Alexa Fluor 594 were excited with a 405-nm laser diode, 488-nm argon laser, and 543-nm HeNe green laser, respectively, and sequential scans were used to maximize signal separation.

Glutathione, NDPK activity, ROS, and protein carbonylation measurements

Total and oxidized glutathione levels were measured using a commercial kit (Cayman Chemical) via an enzymatic recycling method using glutathione reductase. NDPK activity in liver homogenates and hepatocyte lysates was measured by continuous spectrophotometric rate determination using a three-step reaction with ATP, thymidine 5′-diphosphate, phosphoenolpyruvate, pyruvate kinase, and β-NADH. The extinction coefficient of β-NADH at 340 nm (6.22) was used to calculate kinase activity. For ROS measurement, untreated and DDC-treated hepatocytes were loaded with 10 µM CM-H_2DCFDA (Invitrogen) for 20 min, washed, and then mounted in ProLong Gold with DAPI and immediately imaged by confocal microscopy as described in the previous section. Protein carbonylation was measured using a commercial kit (Cell Biolabs, Inc.).

Data analysis

The graph data were presented and statistically analyzed using Prism 5 software (GraphPad Software). Photoshop (CS2; Adobe) was used to

quantify ROS by measuring the green channel (ROS) signal intensity from 15 cells of each treatment condition and dividing by the image areas (in pixels).

Online supplemental material

Fig. S1 shows strain differences in PRDX6 modification and total protein carbonylation in C3H and C57BL livers. Fig. S2 shows a strain comparison of Cyp2e1 levels, ductal proliferation, and glutathione levels. Fig. S3 shows quantification of the immunoblotting data shown in Fig. 7. Table S1 shows relative mRNA expression of selected genes in untreated and DDC-treated C3H and C57BL mice. Table S2 lists the primers used for quantitative real-time PCR. Online supplemental material is available at http://www.jcb.org/cgi/content/full/jcb.201102142/DC1.

This study was supported by National Institutes of Health grants DK52951 (to M. Bishr Omary) and DK34933 (to the University of Michigan), the Department of Veterans Affairs (M. Bishr Omary), and by a University of Michigan Postdoctoral Translational Scholars Program Award (to N.T. Snider) from the National Center for Research Resources grant UL1RR024986 (to the University of Michigan).

Submitted: 28 February 2011
Accepted: 12 September 2011

References

Aithal, G.P., J.A. Thomas, P.V. Kaye, A. Lawson, S.D. Ryder, I. Spendlove, A.S. Austin, J.G. Freeman, L. Morgan, and J. Webber. 2008. Randomized, placebo-controlled trial of pioglitazone in nondiabetic subjects with non-alcoholic steatohepatitis. *Gastroenterology*. 135:1176–1184. http://dx.doi.org/10.1053/j.gastro.2008.06.047

Anstee, Q.M., A.K. Daly, and C.P. Day. 2011. Genetics of alcoholic and non-alcoholic fatty liver disease. *Semin. Liver Dis.* 31:128–146. http://dx.doi.org/10.1055/s-0031-1276643

Arnaud-Dabernat, S., K. Masse, M. Smani, E. Peuchant, M. Landry, P.M. Bourbon, R. Le Floch, J.Y. Daniel, and M. Larou. 2004. Nm23-M2/NDP kinase B induces endogenous c-myc and nm23-M1/NDP kinase A overexpression in BAF3 cells. Both NDP kinases protect the cells from oxidative stress-induced death. *Exp. Cell Res.* 301:293–304. http://dx.doi.org/10.1016/j.yexcr.2004.07.026

Askanas, V., W.K. Engel, and A. Nogalska. 2009. Inclusion body myositis: A degenerative muscle disease associated with intra-muscle fiber multi-protein aggregates, proteasome inhibition, endoplasmic reticulum stress and decreased lysosomal degradation. *Brain Pathol.* 19:493–506. http://dx.doi.org/10.1111/j.1750-3639.2009.00290.x

Beck, J.A., S. Lloyd, M. Hafezparast, M. Lennon-Pierce, J.T. Eppig, M.F. Festing, and E.M. Fisher. 2000. Genealogies of mouse inbred strains. *Nat. Genet.* 24:23–25. http://dx.doi.org/10.1038/71641

Berg, J.M., J.L. Tymoczko, and L. Stryer. 2002. Biochemistry. W.H. Freeman, New York. 1050 pp.

Boissan, M., S. Dabernat, E. Peuchant, U. Schlattner, I. Lascu, and M.L. Lacombe. 2009. The mammalian Nm23/NDPK family: From metastasis control to cilia movement. *Mol. Cell. Biochem.* 329:51–62. http://dx.doi.org/10.1007/s11010-009-0120-7

Braun, S., C. Mauch, P. Boukamp, and S. Werner. 2007. Novel roles of NM23 proteins in skin homeostasis, repair and disease. *Oncogene*. 26:532–542. http://dx.doi.org/10.1038/sj.onc.1209822

Cederbaum, A.I., Y. Lu, and D. Wu. 2009. Role of oxidative stress in alcohol-induced liver injury. *Arch. Toxicol.* 83:519–548. http://dx.doi.org/10.1007/s00204-009-0432-0

Chowdhury, I., Y. Mo, L. Gao, A. Kazi, A.B. Fisher, and S.I. Feinstein. 2009. Oxidant stress stimulates expression of the human peroxiredoxin 6 gene by a transcriptional mechanism involving an antioxidant response element. *Free Radic. Biol. Med.* 46:146–153. http://dx.doi.org/10.1016/j.freeradbiomed.2008.09.027

Colell, A., J.E. Ricci, S. Tait, S. Milasta, U. Maurer, L. Bouchier-Hayes, P. Fitzgerald, A. Guio-Carrion, N.J. Waterhouse, C.W. Li, et al. 2007. GAPDH and autophagy preserve survival after apoptotic cytochrome c release in the absence of caspase activation. *Cell*. 129:983–997. http://dx.doi.org/10.1016/j.cell.2007.03.045

Cortez-Pinto, H., A. Baptista, M.E. Camilo, and M.C. De Moura. 2003. Nonalcoholic steatohepatitis—a long-term follow-up study: comparison with alcoholic hepatitis in ambulatory and hospitalized patients. *Dig. Dis. Sci.* 48:1909–1913. http://dx.doi.org/10.1023/A:1026152415917

Ebert, B., M. Kisiela, P. Malátková, Y. El-Hawari, and E. Maser. 2010. Regulation of human carbonyl reductase 3 (CBR3; SDR21C2) expression by Nrf2 in cultured cancer cells. *Biochemistry*. 49:8499–8511. http://dx.doi.org/10.1021/bi100814d

Eruslanov, E., and S. Kusmartsev. 2010. Identification of ROS using oxidized DCFDA and flow-cytometry. *Methods Mol. Biol.* 594:57–72. http://dx.doi.org/10.1007/978-1-60761-411-1_4

Fleming, K.A., and J.O. McGee. 1984. Alcohol induced liver disease. *J. Clin. Pathol.* 37:721–733. http://dx.doi.org/10.1136/jcp.37.7.721

Gerber, M.A., W. Orr, H. Denk, F. Schaffner, and H. Popper. 1973. Hepatocellular hyalin in cholestasis and cirrhosis: Its diagnostic significance. *Gastroenterology*. 64:89–98.

Goldfarb, L.G., and M.C. Dalakas. 2009. Tragedy in a heartbeat: malfunctioning desmin causes skeletal and cardiac muscle disease. *J. Clin. Invest.* 119:1806–1813. http://dx.doi.org/10.1172/JCI38027

Gramlich, T., D.E. Kleiner, A.J. McCullough, C.A. Matteoni, N. Boparai, and Z.M. Younossi. 2004. Pathologic features associated with fibrosis in nonalcoholic fatty liver disease. *Hum. Pathol.* 35:196–199. http://dx.doi.org/10.1016/j.humpath.2003.09.018

Gruber, C.W., M. Cemazar, B. Heras, J.L. Martin, and D.J. Craik. 2006. Protein disulfide isomerase: The structure of oxidative folding. *Trends Biochem. Sci.* 31:455–464. http://dx.doi.org/10.1016/j.tibs.2006.06.001

Hanada, S., P. Strnad, E.M. Brunt, and M.B. Omary. 2008. The genetic background modulates susceptibility to mouse liver Mallory-Denk body formation and liver injury. *Hepatology*. 48:943–952. http://dx.doi.org/10.1002/hep.22436

Hanada, S., N.T. Snider, E.M. Brunt, P.F. Hollenberg, and M.B. Omary. 2010. Gender dimorphic formation of mouse Mallory-Denk bodies and the role of xenobiotic metabolism and oxidative stress. *Gastroenterology*. 138:1607–1617. http://dx.doi.org/10.1053/j.gastro.2009.12.055

Hara, M.R., N. Agrawal, S.F. Kim, M.B. Cascio, M. Fujimuro, Y. Ozeki, M. Takahashi, J.H. Cheah, S.K. Tankou, L.D. Hester, et al. 2005. S-nitrosylated GAPDH initiates apoptotic cell death by nuclear translocation following Siah1 binding. *Nat. Cell Biol.* 7:665–674. http://dx.doi.org/10.1038/ncb1268

Harada, M., S. Hanada, D.M. Toivola, N. Ghori, and M.B. Omary. 2008. Autophagy activation by rapamycin eliminates mouse Mallory-Denk bodies and blocks their proteasome inhibitor-mediated formation. *Hepatology*. 47:2026–2035. http://dx.doi.org/10.1002/hep.22294

Jeong, J.Y., Y. Wang, and A.J. Sytkowski. 2009. Human selenium binding protein-1 (hSP56) interacts with VDU1 in a selenium-dependent manner. *Biochem. Biophys. Res. Commun.* 379:583–588. http://dx.doi.org/10.1016/j.bbrc.2008.12.110

Klaassen, C.D., and S.A. Reisman. 2010. Nrf2 the rescue: Effects of the antioxidative/electrophilic response on the liver. *Toxicol. Appl. Pharmacol.* 244:57–65. http://dx.doi.org/10.1016/j.taap.2010.01.013

Kornberg, M.D., N. Sen, M.R. Hara, K.R. Juluri, J.V. Nguyen, A.M. Snowman, L. Law, L.D. Hester, and S.H. Snyder. 2010. GAPDH mediates nitrosylation of nuclear proteins. *Nat. Cell Biol.* 12:1094–1100. http://dx.doi.org/10.1038/ncb2114

Ku, N.O., J.K. Lim, S.M. Krams, C.O. Esquivel, E.B. Keeffe, T.L. Wright, D.A. Parry, and M.B. Omary. 2005. Keratins as susceptibility genes for end-stage liver disease. *Gastroenterology*. 129:885–893. http://dx.doi.org/10.1053/j.gastro.2005.06.065

Lanfear, J., J. Fleming, M. Walker, and P. Harrison. 1993. Different patterns of regulation of the genes encoding the closely related 56 kDa selenium- and acetaminophen-binding proteins in normal tissues and during carcinogenesis. *Carcinogenesis*. 14:335–340. http://dx.doi.org/10.1093/carcin/14.3.335

Lee, E., J. Jeong, S.E. Kim, E.J. Song, S.W. Kang, and K.J. Lee. 2009. Multiple functions of Nm23-H1 are regulated by oxido-reduction system. *PLoS ONE*. 4:e7949. http://dx.doi.org/10.1371/journal.pone.0007949

Liem, R.K., and A. Messing. 2009. Dysfunctions of neuronal and glial intermediate filaments in disease. *J. Clin. Invest.* 119:1814–1824. http://dx.doi.org/10.1172/JCI38003

Marouga, R., S. David, and E. Hawkins. 2005. The development of the DIGE system: 2D fluorescence difference gel analysis technology. *Anal. Bioanal. Chem.* 382:669–678. http://dx.doi.org/10.1007/s00216-005-3126-3

Mohanty, S.R., T.N. Troy, D. Huo, B.L. O'Brien, D.M. Jensen, and J. Hart. 2009. Influence of ethnicity on histological differences in non-alcoholic fatty liver disease. *J. Hepatol.* 50:797–804. http://dx.doi.org/10.1016/j.jhep.2008.11.017

Muchowski, P.J., and J.L. Wacker. 2005. Modulation of neurodegeneration by molecular chaperones. *Nat. Rev. Neurosci.* 6:11–22. http://dx.doi.org/10.1038/nrn1587

Nakajima, H., W. Amano, A. Fujita, A. Fukuhara, Y.T. Azuma, F. Hata, T. Inui, and T. Takeuchi. 2007. The active site cysteine of the proapoptotic protein glyceraldehyde-3-phosphate dehydrogenase is essential in oxidative stress-induced aggregation and cell death. *J. Biol. Chem.* 282:26562–26574. http://dx.doi.org/10.1074/jbc.M704199200

Nakajima, H., W. Amano, T. Kubo, A. Fukuhara, H. Ihara, Y.T. Azuma, H. Tajima, T. Inui, A. Sawa, and T. Takeuchi. 2009. Glyceraldehyde-3-phosphate dehydrogenase aggregate formation participates in oxidative stress-induced cell death. *J. Biol. Chem.* 284:34331–34341. http://dx.doi.org/10.1074/jbc.M109.027698

Nguyen, G.C., and P.J. Thuluvath. 2008. Racial disparity in liver disease: Biological, cultural, or socioeconomic factors. *Hepatology*. 47:1058–1066. http://dx.doi.org/10.1002/hep.22223

Ou, X.M., C.A. Stockmeier, H.Y. Meltzer, J.C. Overholser, G.J. Jurjus, L. Dieter, K. Chen, D. Lu, C. Johnson, M.B. Youdim, et al. 2010. A novel role for glyceraldehyde-3-phosphate dehydrogenase and monoamine oxidase B cascade in ethanol-induced cellular damage. *Biol. Psychiatry*. 67:855–863. http://dx.doi.org/10.1016/j.biopsych.2009.10.032

Porat, A., Y. Sagiv, and Z. Elazar. 2000. A 56-kDa selenium-binding protein participates in intra-Golgi protein transport. *J. Biol. Chem.* 275:14457–14465. http://dx.doi.org/10.1074/jbc.275.19.14457

Postel, E.H., S.J. Berberich, S.J. Flint, and C.A. Ferrone. 1993. Human c-myc transcription factor PuF identified as nm23-H2 nucleoside diphosphate kinase, a candidate suppressor of tumor metastasis. *Science*. 261:478–480. http://dx.doi.org/10.1126/science.8392752

Promrat, K., G. Lutchman, G.I. Uwaifo, R.J. Freedman, A. Soza, T. Heller, E. Doo, M. Ghany, A. Premkumar, Y. Park, et al. 2004. A pilot study of pioglitazone treatment for nonalcoholic steatohepatitis. *Hepatology*. 39:188–196. http://dx.doi.org/10.1002/hep.20012

Räisänen, S.R., P. Lehenkari, M. Tasanen, P. Rahkila, P.L. Härkönen, and H.K. Väänänen. 1999. Carbonic anhydrase III protects cells from hydrogen peroxide-induced apoptosis. *FASEB J.* 13:513–522.

Rakoski, M.O., M.B. Brown, R.J. Fontana, H.L. Bonkovsky, E.M. Brunt, Z.D. Goodman, A.S. Lok, and M.B. Omary; HALT-C Trial Group. 2011. Mallory-Denk bodies are associated with outcomes and histologic features in patients with chronic hepatitis C. *Clin. Gastroenterol. Hepatol.* 9:902–909. http://dx.doi.org/10.1016/j.cgh.2011.07.006

Sanyal, A.J., N. Chalasani, K.V. Kowdley, A. McCullough, A.M. Diehl, N.M. Bass, B.A. Neuschwander-Tetri, J.E. Lavine, J. Tonascia, A. Unalp, et al; NASH CRN. 2010. Pioglitazone, vitamin E, or placebo for nonalcoholic steatohepatitis. *N. Engl. J. Med.* 362:1675–1685. http://dx.doi.org/10.1056/NEJMoa0907929

Sen, N., M.R. Hara, M.D. Kornberg, M.B. Cascio, B.I. Bae, N. Shahani, B. Thomas, T.M. Dawson, V.L. Dawson, S.H. Snyder, and A. Sawa. 2008. Nitric oxide-induced nuclear GAPDH activates p300/CBP and mediates apoptosis. *Nat. Cell Biol.* 10:866–873. http://dx.doi.org/10.1038/ncb1747

Sen, N., M.R. Hara, A.S. Ahmad, M.B. Cascio, A. Kamiya, J.T. Ehmsen, N. Agrawal, L. Hester, S. Doré, S.H. Snyder, and A. Sawa. 2009. GOSPEL: A neuroprotective protein that binds to GAPDH upon S-nitrosylation. *Neuron*. 63:81–91. http://dx.doi.org/10.1016/j.neuron.2009.05.024

Smith, D.M., N. Benaroudj, and A. Goldberg. 2006. Proteasomes and their associated ATPases: A destructive combination. *J. Struct. Biol.* 156:72–83. http://dx.doi.org/10.1016/j.jsb.2006.04.012

Snider, N.T., S.V. Weerasinghe, J.A. Iñiguez-Lluhí, H. Herrmann, and M.B. Omary. 2011. Keratin hypersumoylation alters filament dynamics and is a marker for human liver disease and keratin mutation. *J. Biol. Chem.* 286:2273–2284. http://dx.doi.org/10.1074/jbc.M110.171314

Steeg, P.S., and D. Theodorescu. 2008. Metastasis: A therapeutic target for cancer. *Nat. Clin. Pract. Oncol.* 5:206–219. http://dx.doi.org/10.1038/ncponc1066

Su, T., and D.J. Waxman. 2004. Impact of dimethyl sulfoxide on expression of nuclear receptors and drug-inducible cytochromes P450 in primary rat hepatocytes. *Arch. Biochem. Biophys.* 424:226–234. http://dx.doi.org/10.1016/j.abb.2004.02.008

Tristan, C., N. Shahani, T.W. Sedlak, and A. Sawa. 2011. The diverse functions of GAPDH: Views from different subcellular compartments. *Cell. Signal.* 23:317–323. http://dx.doi.org/10.1016/j.cellsig.2010.08.003

Whalen, R., and T.D. Boyer. 1998. Human glutathione S-transferases. *Semin. Liver Dis.* 18:345–358. http://dx.doi.org/10.1055/s-2007-1007169

Wong, C.M., A.K. Cheema, L. Zhang, and Y.J. Suzuki. 2008. Protein carbonylation as a novel mechanism in redox signaling. *Circ. Res.* 102:310–318. http://dx.doi.org/10.1161/CIRCRESAHA.107.159814

Wong, C.M., L. Marcocci, L. Liu, and Y.J. Suzuki. 2010. Cell signaling by protein carbonylation and decarbonylation. *Antioxid. Redox Signal.* 12:393–404. http://dx.doi.org/10.1089/ars.2009.2805

Wood, Z.A., L.B. Poole, and P.A. Karplus. 2003. Peroxiredoxin evolution and the regulation of hydrogen peroxide signaling. *Science*. 300:650–653. http://dx.doi.org/10.1126/science.1080405

Wu, Y., S.I. Feinstein, Y. Manevich, I. Chowdhury, J.H. Pak, A. Kazi, C. Dodia, D.W. Speicher, and A.B. Fisher. 2009. Mitogen-activated protein kinase-mediated phosphorylation of peroxiredoxin 6 regulates its phospholipase A(2) activity. *Biochem. J.* 419:669–679. http://dx.doi.org/10.1042/BJ20082061

Yokoo, H., T.R. Harwood, D. Racker, and S. Arak. 1982. Experimental production of Mallory bodies in mice by diet containing 3,5-diethoxycarbonyl-1, 4-dihydrocollidine. *Gastroenterology*. 83:109–113.

Zatloukal, K., S.W. French, C. Stumptner, P. Strnad, M. Harada, D.M. Toivola, M. Cadrin, and M.B. Omary. 2007. From Mallory to Mallory-Denk bodies: What, how and why? *Exp. Cell Res.* 313:2033–2049. http://dx.doi.org/10.1016/j.yexcr.2007.04.024